Assessment of Wind Energy Resource Potential for Future Human Missions to Mars

Victoria Hartwick (victoria.hartwick@nasa.gov)
NASA Ames Research Center https://orcid.org/0000-0002-2082-8986
Owen Toon
University of Colorado-Boulder
Julie Lundquist
University of Colorado-Boulder
Olivia Pierpaoli
University of Washington-Seattle
Melinda Kahre

Article

Keywords:

Posted Date: April 15th, 2022

DOI: https://doi.org/10.21203/rs.3.rs-1510777/v1

Version of Record: A version of this preprint was published at Nature Astronomy on December 19th, 2022. See the published version at https://doi.org/10.1038/s41550-022-01851-4.

Abstract

Future crewed missions to Mars will require sustained sources of energy, including solar, nuclear and wind energy. Using a state-of-the-art Mars general circulation model, we analyze the Martian wind potential and calculate its spatial and temporal variability. Here we show that wind speeds at several proposed landing sites are sufficiently fast to provide an alternative energy source, which could be particularly important at night, at middle to polar latitudes and during dust storms. Several regions show promising wind energy resource potential. These findings demonstrate that wind energy represents a valuable energy resource that compensates for diurnal and seasonal reductions in solar power and offers an opportunity for wind turbine technological advancement and engineering creativity with the aim of extracting more power from Mars winds.

Main Text

Future crewed missions to Mars will require surface habitats and scientific instrumentation with sustained and redundant sources of energy. Site selection and risk assessment strategies must critically assess the available energy resources on both long-term and shorter diurnal and seasonal timescales. The driving principle behind site selection for human missions to Mars thus far has centered around physical resource allocation and, in particular, the surface or near-surface availability of water ice and the distribution of volcanic lava tubes that can serve as long term habitats. Mandates to "follow the water" and "find shelter" direct attention to regions with evidence of surface liquid water as in recurring slope lineae in the Valles Marineris, Mawrth Vallis, and midlatitudes (*1-3*), close to large near-subsurface ice deposits as in the Northern Hemisphere polar and midlatitudes (*4-8*), or within large scale magma deposits such as along the Tharsis volcanic plateaus (*9,10*).

However, regions of scientific interest or with the greatest diversity of physical resources may not overlap with regions with the highest energy production potential. In particular, the very characteristics that make the current class of proposed landing sites or regions attractive, including their geology, theorized mineralogical history and availability of local resources, limit traditional energy resources. For example, energy limitations occur in the polar and midlatitudes where solar energy varies dramatically with season or in dusty corridors in the Northern and Southern Hemisphere where solar energy decreases proportionally with atmospheric dust. While robotic missions historically have relied on either solar or nuclear power, both energy sources have inherent risks and weaknesses. Solar energy requires that a sufficient proportion of solar radiation reaches the planetary surface on a per-sol basis. As on Earth, available solar power varies with time of day, season, and latitude. If potential landing sites move poleward where water ice deposits are more readily available, seasonal variability of solar energy increases and the need for a secondary energy resource is amplified. Depending on both the season and location of future landing sites, atmospheric optical depths can reach prohibitively high values at which solar energy no longer represents a feasible energy source on short to multi-sol timescales. Dust accumulation on the surface of solar cells will further decrease efficiency and necessitate periodic cleaning of solar panels to maximize energy outputs. Further, solar energy is necessarily limited by time of day; solar cells are not operational during nighttime hours while mission and life support systems remain critical. Remediation of seasonal and shorter-term, multi-sol power outages with nuclear power has its own risks, such as the safety of nuclear devices near human settlements over extended periods of time. If mission plans prioritize local physical resources and scientific interest above theoretical solar energy yields and if energy storage is limited, engineering multiple redundant energy sources will be critical. In this research we propose the use of wind power as an additional energy resource for future human missions to Mars.

Wind energy has historically been disregarded as a potential source of alternative energy for missions to Mars due to Mars' low atmospheric density. The density of the Martian atmosphere is approximately one hundredth the density of Earth's atmosphere, and, as a result, the power associated with a fixed wind speed is reduced by approximately 99%. This reduction in the energetic return from winds of all magnitudes and the hypothesized lack of high-velocity wind gusts in the lower 50-100 m of the Martian atmosphere, has made wind energy generally unappealing. However, first assessments of the Martian wind power were based primarily on Viking diurnal wind profiles, or on a global average understanding of wind speeds that disregarded local meteorology or that assessed energy production potential at one location only (*11-17*). For example, although the simulated global average surface wind speed is approximately 12.4 m/s (very near or just below the 8-20 m/s Mars atmosphere density-adjusted cut-in or activation wind speed for most turbines), wind speeds vary significantly with topography, season, time of day and in response to changing surface thermal properties and snow/ice cover. Notably, many of the proposed landing sites for future crewed missions to Mars are in regions of high topographic relief or regions with thermal variation that act to enhance wind speeds well above the global average.

Turbine technology has also advanced significantly in the last decade. In general, more power can be generated at weaker, more common wind speeds that require lower hub heights or that occur in regions that would have previously been considered poor candidates for wind development. Both factors favor a Martian application. At the same time, a greater number of options for turbine types (e.g., bladed versus bladeless; vertical-axis and eddy turbines versus horizontal-axis turbines; variations to blade shape, weight, and length; and airborne or balloon turbines), hub heights, and sizes are available. These options include microturbines intended for battery charging or as backup

generators for boats or campers and industry-scale multimegawatt turbines, that generate enough energy to power tens of thousands of households (*18*). Because weight is the major concern for any instrument that must be transported from Earth to Mars, these turbines provide multiple weight and size options depending on the energetic requirements for each mission. For example, a vertical-axis, microturbine would generate sufficient energy to have powered the Mars Opportunity rover during the Mars Year (MY) 34 global dust storm and weighs only 28 kg. By contrast, the Enercon E33 turbine, a medium-scale turbine that has been used at Mars analog sites in Antarctica, could feasibly generate power for an entire human mission but is more massive (potentially up to several tons). Further, while the turbine nacelle would likely need to be constructed on Earth and transported to Mars, blades are typically composed of fiberglass and therefore could potentially be fabricated in situ, substantially reducing the overall transported size and weight. Likewise, some turbine components, including the tower, rotor hub, gearbox, and frame, have been constructed out of aluminum alloy versus the traditional steel (*19,20*). Fabric-covered blades have also been proposed (*21*). The use of alternative turbine types (e.g., airborne or bladeless) or placing turbines on rovers or crater rims would reduce the overall height of towers and could therefore further reduce the total weight (*22*). It is beyond the scope of this work to assess each turbine or the ultimate feasibility of turbine transport and construction; rather, we intend this article to serve as a proof of concept. Although turbines are more massive than solar panels, we argue that they represent a useful and reliable energy source particularly at night and in the winter hemisphere midlatitudes. We encourage future work on this topic, including in-depth engineering studies that reduce turbine weight and maximize efficiency.

Because this study represents an initial look at the global wind power potential for Mars using a detailed Martian climate model, the most important factor to consider is the overall power availability rather than the specific power that could be extracted by a specific turbine. The majority of our analysis therefore utilizes the wind power density (WPD), which represents the maximum possible power production per unit area for an idealized or 100% efficient turbine. The WPD has the added benefit of being technology-agnostic and therefore remains useful as turbine technology continues to advance. Additionally, the WPD is the most straightforward tool to help compare wind and solar energy without complicating considerations of array or turbine size and efficiency. Because concrete examples are also useful, we calculate the power return from a base-case turbine, the Enercon E33, and three additional turbines ranging from microscale to industry scale. We compare the energy generated by turbines alone and in combination with a solar array to the theorized energy requirements for a crewed mission to Mars and use these metrics to locate potential regions of interest for future landing sites.

The Wind Power Density Demonstrates the Maximum Available Energy

Wind power is proportional to the atmospheric density and the wind speed u^3 (Eqn. 1). Mars has a thin atmosphere and, in general, weaker winds than on Earth. As a result, power return from any wind-based energy system will be proportionally less. For example, for the same wind speed, a perfect turbine on Mars will produce only 1% the power of the same turbine on Earth. Figure 1 shows the annual average WPD at 5, 30, 50, and 100 m for a non-dust storm year. In general, wind speeds increase with height and therefore, the power potential increases as the turbine hub height (or altitude of the turbine blades) increases. Offshore wind turbines on Earth regularly have hub heights as high as 100-150 m, however, it is likely that engineering or transport restrictions will ultimately limit the maximum hub height on Mars to lower altitudes. We therefore choose a moderate hub height altitude of 50 m for our base analysis. However, for energy calculations that use turbine specific power curves (Data S1-S4), we vary hub height from 5 to 100 m to match individual turbine specifications.

$$WPD = \frac{1}{2}\rho u^3 \qquad \text{Eqn. 1}$$

At all altitudes, baroclinic wave activity drives high wind speeds adjacent to/associated with the winter hemisphere polar vortex and the descending branch of the seasonal Hadley circulation. Baroclinic waves travel towards the equator and summer hemisphere through north/south topographic channels. As a result, the WPD is highest along regions with large topographic gradients such as along crater rims and throughout the volcanic highlands. Wind power is similarly enhanced in regions with high thermal variability. For example, during Northern Hemisphere winter, winds blow from cooler surface ice deposits to warm regolith. This effect, analogous to a "sea breeze," may be particularly important at proposed high-latitude base camps adjacent to seasonal ice deposits. In several locations, the annual average wind power can exceed available solar power by up to 3.4 times (Fig. 1e). While the Mars annual average WPD is low (typically < 100 W/m^2), on shorter timescales and in some locations, the WPD can exceed 3,000 W/m^2. We also note that for the purposes of short-term human missions to Mars, the total estimated power requirement is just 20-40 kW, within feasible energy production rates for a standard turbine with a blade length of 5-10 m across a large fraction of the Mars surface.

Wind Power Varies Seasonally, Diurnally and Due to Dust Storms

Temporal averaging used to produce the annual average WPD will mask the predicted resource potential in regions with large seasonal and/or diurnal variability. Figure 2 shows the wind and solar power density at the Mars cardinal seasons. We draw particular attention to the potential solar and wind energy yields in the polar and midlatitudes in the solstitial winter hemispheres. When solar energy is seasonally reduced (Fig. 2a,c), wind energy represents an important energy backup. Fortuitously, when wind energy is potentially most important, wind energy yields are also at their highest - for example, as along the Hellas (42.74°S,70.5°E) and Argyre (49°S,318°E) impact basins at the solar longitude 90° (L_s~90°, time of the northern summer solstice) and northwards of approximately 40°N latitude at L_s~270° (northern winter solstice). In these regions, the seasonal average wind power regularly exceeds 100 W/m^2 while solar power is reduced to values below 25-50 W/m^2. To more clearly demonstrate this seasonal cycling between solar and wind power, we plot the wind in 5° longitude bands and zonal average solar power versus time for several latitudes (Fig. S1). Wind power more than compensates for reduced solar power in the winter hemisphere. Reductions in the Southern Hemisphere solar power after L_s~180° (northern autumnal equinox) are associated with regional storm activity (Fig. S1d,e).

During global dust storm years, higher atmospheric dust levels are positively correlated with greater wind power production. For example, in Fig. 3 we show the difference in WPD for MY28 (a global dust storm year) versus MY24 (a typical, non-global dust storm year). At the time of the most intense dust storm activity (L_s=260°-280°), wind power in MY28 exceeds MY24 wind power production by greater than 60 W/m^2 on average and by up to 300 W/m^2. This elevated wind power occurs simultaneously with an approximate 50 W/m^2 global decrease in solar power due to high atmospheric dust opacity. The extent to which turbines remain efficient if dust accumulates during local storms requires additional study (*23*).

The most fundamental limitation for solar power development is its diurnal variability. If excess energy cannot be easily stored, then power redundancies during nighttime hours will be required. Wind energy is particularly suited to address this problem because winds on Mars are generally fastest at dawn and dusk. In Fig. 4 we show the annual average day and night WPD and the ratio. Night is defined in our simulations as local time (LT) 8.5-16.5. Nighttime wind power exceeds the available daytime wind energy by up to a factor of 57.5 and on average by a factor of ~2. Figure S2 shows the annual average solar and wind power density in one-hour intervals. Solar power exceeds 140 W/m^2 during daytime hours (~8.5-16.5 LT) while wind power maximizes at night (~17.5-7.5 LT). Wind power could be a valuable resource, particularly at night, during local and global dust events and seasonally in the midlatitudes and polar regions.

Enercon E33 Power and Energy Calculations

Wind turbines are not perfectly efficient, and the amount of energy that can be extracted from wind fields will not exactly match the WPD. Importantly, power depends on turbine efficiency and the area swept by its blades (Eqn 2). Here, is the atmospheric density, u is the wind speed at the turbine hub or blade height, A is the rotor swept area, and C_p is the wind-speed-dependent power coefficient (*24*).

$$Power = \frac{1}{2}\rho u^3 C_p A \qquad \text{Eqn. 2}$$

To account for turbine-specific engineering with complex efficiency factors that shift energy production from Eqn, 2 (e.g., at different wind speeds), turbine documentation includes the measured power curve. The power curve provides the anticipated power return in wind speed bins at standard sea-level conditions (Data S1-S4). Power curves are unique to each turbine and consider variations of the power coefficient with wind speed as well as threshold wind speeds required to initiate (cut in) and stop (cut off) energy production. While these values will likely differ under Martian conditions, they represent a meaningful improvement over theoretical power yields that are highly generalizable but are often inaccurate (*25*). For example, the calculated power using Eqn. 2 underpredicts the power generation at low wind speeds and overpredicts the power generation at high wind speeds near the cut-off threshold (Fig. S3). To better assess realistic power returns at Mars, we use a power curve from the Enercon E33 wind turbine. The Enercon E33 turbine is currently used at the Ross Island Wind Farm, an analogue site for present-day Mars *(26)*. Turbine specifications are summarized in Table S1. Figure S4 shows the annual energy production (AEP), or the total energy at each location summed over the duration of the Mars year. As a point of reference, we compare this value with

the approximate solar panel array dimensions required to generate the same total annual energy. In regions with the highest wind AEP, solar arrays would need to exceed 7,000 m^2. The average AEP would require array sizes greater than 600 m^2.-

Load Duration Curves: Do turbines produce energy in bursts or continuously?

Neither the WPD nor AEP quantify the temporal distribution of energy production that will be critical for supporting long-term human missions. For example, two sites with the same AEP may generate energy very differently: slowly over the entire year or in high magnitude but sporadic bursts. To better understand the stability of wind resources over the Martian year, we calculate the power duration curves at proposed landing sites.

The power duration curve measures the percentage of time at which a turbine is functioning at some percentage of its rated power. Most turbines operate with varying efficiency throughout the year. The optimal operational capacity will vary with each turbine, site and mission. For example, using a larger turbine with a higher rated power that operates at a lower capacity may be more desirable and ultimately generate more power than using a small turbine that operates near capacity. Therefore, when evaluating power duration in this work, we focus on the distribution of energy production (e.g., smooth or stochastic) rather than the exact capacity factor.

We show the global average annual and seasonal power duration curves as well as the power duration curves at three potential landing sites in Fig. S5. The global average load duration (Fig. S5a) is generally low, operating at less than ~2%-4% capacity for 50% of the time. For the Enercon E33 wind turbine, this translates to an average operational power of approximately 10 kW. As expected, load durations vary substantially with season and location. At Protonilus Mensae (38°N, 48°E), a proposed landing site in the Northern Hemisphere midlatitudes, the capacity factor exceeds 20% and increases up to 50%-70% for significant fractions of time, particularly during L_s=180°, 270° and 0°, when solar power yields are reduced. Seasonal curves show the time average over 20° L_s or approximately 30-50 sols. Power duration curves suggest that wind power generation occurs at low levels but consistently rather than sporadically over the Mars year. This is critical because energy storage capabilities on Mars are still limited. Consistent, low-power generation makes wind energy more valuable than significant energy production in short, sporadic bursts.

Potential Regions of Interest for Future Human Missions to Mars

Wind energy will only be useful if it can be produced in regions that are attractive for future human missions. Significant work has already been done to identify potential human landing sites based on geology, resource potential and engineering limitations. The NASA Human Landing Site Study (HLS2) identified 50 potential regions of interest (ROI) based on these criteria. The study did not consider the energy availability of each region beyond coarse latitude restrictions to avoid polar night or excessive terrain shading that would limit agricultural development.

Numerous studies have additionally assessed the energy requirements for human missions of varied size and duration. The most comprehensive of these studies (*27*) calculates a 24-35 kW surface system power requirement to support a 6-crew, 500-sol mission. Red squares in Fig. 5 shows locations where the diurnal average wind power produced by the Enercon E33 turbine in MY24 exceeds this limit at all simulated times throughout the year. At these locations, wind energy is therefore theoretically sufficient to power the entire mission on its own. Any human mission to Mars will include multiple redundant energy sources, including solar and nuclear. We therefore similarly assess regions of the planet where our base turbine could power different portions of the mission - for example, the surface habitat and life support systems (12.1-17.258 kW) or scientific instrumentation (2.2 kW) (*27*).

The major advantage of wind energy is its availability as a complement to solar during global dust storms, seasonally in the winter middle to high latitudes, or at night (Fig. S6). At winter solstices, wind energy is a valuable resource particularly near the poles and midlatitudes. The increase in locations with high wind energy is in part due to the reduced time period over which the energy resource is required to stay stable (here, approximately 50 sol or 20° L_s compared with Fig. 5, which covers the entire Mars year). However, elevated energy levels in the winter hemisphere correspond to seasonally enhanced wind speeds. Despite the clear advantage of local water resources, many sites above these latitudes have been dismissed due to solar energetic limitations during polar night. We demonstrate that if the availability of water outweighs other challenges, wind energy could act as the dominant energy source when solar energy is seasonally depleted, opening a large

fraction of the polar landscape to human exploration. Similarly, wind energy resources maximize at night when solar energy is at its minimum.

To demonstrate the combined resource potential from solar and wind, we show in Fig. 6a-c the percentage of time over the Mars year that power generation exceeds 24kW based on production from the Enercon E33 turbine and a theoretical solar array. We calculate solar power using a solar panel efficiency factor of 0.2, at the high end of the range for commercial technology *(28)* and not accounting for reductions in efficiency due to surface dust accumulation, which can exceed 89% *(29)*. Simulated solar arrays have a total area of 2,500 m^2 based on the 2017 NASA Small Business Innovation Research solicitation (*30*), although they may be smaller (*31,32*, Fig. S7). Solar arrays of this size generate the requisite power about 40% of the time in a broad zonal band from ~60°S to 60°N. This makes sense because solar power generation is unavailable at night (~50% of the time) and is further reduced in the winter hemisphere and during local dust events. The Enercon E33 generates power with equivalent or greater stability (>24 kW for 30%-50% of the year), but peaks are more highly localized. In combination, percentages can rise to over 90%, which indicates that wind power is most active when solar power is reduced, rather than generating useful but redundant power at the same times of the day and year.

Based on these metrics, we identify the most favorable locations for wind energy development both on its own and as a complement to seasonally and diurnally varying solar output. Of the 50 ROI identified in the HLS2, a single Enercon E33 turbine at Deuteronilus Mensae 2 (35°N, 23°E), Protonilus Mensae (38°N,48°E), and Ismenius Lacus (29°N,17°E) could produce 24 kW more than 35% of the year (and >75% of the year when combined with solar power) and therefore represent the most attractive sites from a wind resource perspective. A further seven sites generate significant wind energy seasonally and contribute more than 50% of the total power generation either in the winter hemisphere or in the dusty Southern Hemisphere at L_s=270°. Table S2 highlights ROIs from the HLS2 that represent the best candidates for wind energy development. We note that if wind power is used to maintain power for scientific instrumentation (2.2kW), only 10 ROI are excluded by a 50% seasonal wind power time requirement. We also identify several new broad regions of interest for human exploration that generate the mission energy requirements > 40% of the time (or >65% of the time with solar) (a) annually or (b) seasonally and therefore compensate for reduced solar output. Findings are shown in Fig. 6d. Red dots show the HLS2 ROI highlighted in Table S2. Yellow dots show crater ROI where very high resolution or mesoscale simulations are likely necessary to accurately capture topographically influenced wind speeds and theoretical power production. If diurnal slope winds are resolved, these sites may ultimately produce significant amounts of energy via wind turbines. Black and white boxes highlight newly identified regions of interest.

Alternative Turbines

Wind turbine power production will vary with turbine specifications, including turbine hub height, blade area and engineering specifications, that determine cut-in, cut-off, and rated wind speeds as well as the wind-speed-dependent power coefficient. To demonstrate this variability, we include analysis of three additional turbines. The Jacobs 31-20 turbine is the smallest turbine considered here. Its primary use is single-family, local residences or small occupancy power needs. At the other extreme, we also show the power return of an industry-standard 5-MW turbine used in off-shore wind farms on Earth to power large industries or populations centers. The largest turbines on Earth now produce up to 15 MW. Each turbine has different advantages and disadvantages for operation at an interplanetary scale. For example, the National Renewable Energy Laboratory (NREL) 5-MW turbine generates the highest theoretical power by a large margin, however, it is also the largest and most difficult to transport, set up and maintain on Mars.

Table S3 shows the global average AEP for each wind turbine. As expected, smaller turbines with lower hub heights and lesser rated power produce less energy. Similarly, an industrial-scale turbine such as the NREL 5-MW turbine produces large amounts of energy nearly uniformly across the entire Mars surface (Fig. S8). The smallest turbines are best-suited to act as backup power resource for solar arrays, while larger turbines could act as independent power sources. The most important takeaway is that even a small turbine will produce enough energy to power some portion of a human mission to Mars.

In addition to large industrial or household wind turbines, microturbines could potentially act as auxiliary power for scientific instruments or to recharge batteries. For example, we find that the Aeolos-V 300-W turbine could have generated sufficient power to maintain functionality for the solar-powered Opportunity rover during the 2018 (MY34) global dust storm. The Aeolos-V turbine was selected based on its moderate weight and low cut-in wind speed. In theory, it could be mounted directly on the rover, providing a hub height of approximately 5 m. At end of mission, sol 5111, the Opportunity solar panels generated 22 Wh (~0.86 W) (*33*). We simulated the power output of the Aeolos-V turbine at 5

m for the same time period and found a 5-sol average power production of 207 Wh (Fig. S9). This amount of energy would be sufficient to maintain the rover clock (but not drive) through the most intense period of the dust storm or until solar power could be restored.

Conclusion

Wind energy represents a valuable but previously dismissed energy resource for future human missions to Mars, which will be useful as a complementary energy source to solar power. Wind becomes particularly valuable when solar power is reduced, such as at nighttime, during local or large-scale dust events and at higher latitudes that are attractive due to their close proximity to water resources but experience large seasonal variability in solar power. Turbines will need to operate under unique Martian conditions and must be easily transported, constructed and maintained. Significant work is necessary to better understand and assess unique engineering requirements and challenges to wind power. However, using a global model of atmospheric circulation, coupled with analog turbines, we suggest that across large portions of the Mars' surface, wind power is a stable, sustained energy resource over the duration of the Mars' year. Although load durations are generally low, this is preferable to energy production in large magnitude but sporadic bursts that would only exacerbate known energy storage concerns. Based on wind energy analysis we identify 13 new regions of interest for human exploration of Mars and highlight 10 of the 50 previously identified HLS2 regions of interest that have good wind resource potential. The best candidates are Deuteronilus Mensae 2 (35°N, 23°E), Protonilus Mensae (38°N,48°E), and Ismenius Lacus (29°N,17°E).

Methods

Summary of General Circulation Model Set-up

We use the new NASA Ames Mars Global Climate Model (GCM), which couples the National Oceanic and Atmospheric Administration Geophysical Fluid Dynamics Laboratory cubed-sphere finite volume (FV3) dynamical core and physics packages from the NASA Ames Legacy model described in (*34,35*). Simulations are performed with 1x1-degree resolution and 30 vertical atmospheric levels between 724 and 0.35Pa. The model uses topographic, thermal inertia and albedo maps from the Mars Orbiter Laser Altimeter (MOLA) and Viking and Mars Global Surveyor Thermal Emission Spectrometer observations, respectively. The surface roughness is fixed to 0.01 m (*34*). To assess both wind and solar energy resources during a nominal background dust cycle (Mars Year [MY] 24) and during a global storm (MY28), we use dust opacity maps that match the observed dust optical depths from MY24 and MY28 (*36*).

Calculation of Wind Power Density and Turbine Specific Power Output

Diagnostic variables including atmospheric temperature and zonal and meridional wind fields are calculated every 15 minutes and averaged over 5 Mars days (sols) in 1-hour increments to capture diurnal variability and then interpolated to altitude above the surface to assess power outputs at hub heights between 5 and 100 m above the surface. The wind power density and turbine power and energy calculations use the wind speed $(u^2+v^2)^{0.5}$. To calculate power outputs from individual turbines (Table S1) we use power curves, which provide power output versus binned wind speeds (Data S1-S4). Wind speeds are first scaled based on the Martian and Earth atmospheric densities before being used as inputs for the power curve using a simple wind speed transformation to adapt power curves to different sites including high-altitude sites on Earth (Eqn. S1, [*23*]). So, for example, while a 10-m/s wind on Earth will produce 222 kW based on the power curve for a 330-kW turbine, a ~43-m/s wind is required to generate the same power on Mars. Because Mars atmospheric density varies dramatically with location - for example between the Northern and Southern Hemispheres - as well as with time of year, the wind speeds intervals are scaled at each location and model time step.

$$u_{adjusted} = u_{original} \cdot \left(\frac{\rho mars}{\rho earth}\right)^{\frac{1}{3}} \qquad \text{Eqn. S1}$$

Declarations

Acknowledgments

We thank Dr. Clara St. Martin for suggestions during the initial conceptualization of this project.

This work was authored in part by the National Renewable Energy Laboratory, operated by Alliance for Sustainable Energy, LLC, for the U.S. Department of Energy (DOE) under Contract No. DE-AC36-08GO28308. Funding provided by U.S. Department of Energy Office of Energy Efficiency and Renewable Energy Wind Energy Technologies Office and by the National Offshore Wind Research and Development Consortium under Agreement No. CRD-19-16351. The views expressed in the article do not necessarily represent the views of the DOE or the U.S. Government. The U.S. Government retains and the publisher, by accepting the article for publication, acknowledges that the U.S. Government retains a nonexclusive, paid-up, irrevocable, worldwide license to publish or reproduce the published form of this work, or allow others to do so, for U.S. Government purposes.

Funding

National Science Foundation Graduate Research Fellowship, Grant No. 1144083 (VLH)

NASA Postdoctoral Fellowship Program (VLH)

Author contributions

VLH was responsible for the conceptualization, experimental design and primary investigation of the presented research. VLH wrote the original draft and generated visuals. Funding was provided by VLH. Both OBT and JKL helped design the study methodology and reviewed and edited the manuscript. OAP assisted in the investigation and visualization of work.

Competing interests

Authors declare that they have no competing interests.

Data and code availability

The code used to analyze the NASA Ames general circulation model data files is available at https://github.com/alex-kling/amesgcm and https://github.com/vhartwick/Mars-Wind-Energy.

Additional Information

Extended Data is available for this paper. Correspondence and requests for materials should be addressed to Victoria Hartwick (victoria.hartwick@gmail.com). Reprints and permissions information is available at www.nature.com/reprints.

References

1. Stillman, D. E., Michaels, T. I., Grimm, R. I., & Harrison, K. P. New observations of Martian southern mid-latitude recurring slope lineae (RSL) imply formation by freshwater subsurface flows. *Icarus* **223**, 328-341 (2014). doi:10.1016/j.icarus.2014.01.017.
2. Stillman, D. E., Micheals, T. I., & Grimm, R. E. Characteristics of the numerous and widespread recurring slope lineae (RSL) in Valles Marineris, Mars. *Icarus* **285**, 195-210 (2017). doi:10.1016/j.icarus.2016.10.025.
3. Bhardwaj, A., Sam, L., Martin-Torres, F. J., & Zorzano, M.-P. Discovery of recurring slope lineae candidates in Mawrth Vallis, Mars. *Sci. Rep.* **9**, 2040 (2019). doi:10.1038/s41598-019-39599-z.
4. Bramson, A. M., et al., Widespread excess ice in Arcadia Planitia, Mars. *J. Geophys. Res.* **42**(16), 6566-6574 (2015). doi:10.1002/2015GL064844.

5. Mellon, M. T., Feldman, W. C., & Prettyman, W. C. The presence and stability of ground ice in the Southern Hemisphere of Mars. *Icarus* **169**(2), 324-340 (2004). doi:10.1016/j.icarus.2003.10.022.
6. Dundas, C. M., et al., Widespread exposures of extensive clean shallow ice in the midlatitudes of Mars. *J. Geophys. Res. Planets* **126**(3) (2021). doi:10.1029/2020JE006617.
7. Hibbard, S. M., Williams, N. R., Golombek, M. P., Osinki, G. R., & Godin, E., Evidence for widespread glaciation in Arcadia Planitia, Mars. *Icarus* **359**, 114298 (2021). doi:10.1016/j.icarus.2020.11498.
8. Morgan, G. A., et al., Availability of subsurface water-ice resources in the northern mid-latitudes of Mars. *Nat Astron.* **5**, 230-236 (2021). doi:10.1038/s41550-020-01290-z.
9. Perkins, S., Core Concept: Lava tubes as havens for ancient alien life and future human explorers. *PNAS* **117**(30), 17461-17464 (2020). doi:10.1073/pnas.2012176117.
10. Esmaeili, S., et al., Resolution of lava tubes with ground penetrating radar: The TubeX Project. *J. Geophys. Res. Planets* **125**(5) (2020). doi:10.1029/2019JE006138.
11. Haslach Jr, H. W., Wind energy: A resource for a human mission to Mars. *JBIS* **42**, 171-178 (1989).
12. James, G., Chamitoff, G., & Barker, D., Design and resource requirements for successful wind energy production on Mars, paper presented at the Second International Mars Society Convention, Boulder, CO, 1999. https://citeseerx.ist.psu.edu/viewdoc/download?doi=10.1.1.662.5775&rep=rep1&type=pdf
13. Delgado-Bonal, A., Martín-Torres, F. J., Vázquez-Martín, S., & Zorzano, M.-P., Solar and wind energy potentials for Mars. *Energy* **102**, 550–558 (2016). doi:10.1016/j.energy.2016.02.110
14. Holstein-Rathlou, C., Wind turbine power production under current Martian atmospheric conditions, paper presented at the Mars Workshop on Amazonian Climate, LPIContrib.No.2086 (2018).
15. Lichter, M. D., & Viterna, L. A., "Performance and feasibility analysis of a wind turbine power system for use on Mars", Tech. Rep. NASA/TM-1999-209390, National Aeronautics and Space Administration, Glenn Research Center, 1999; https://ntrs.nasa.gov/api/citations/19990081125/downloads/19990081125.pdf).
16. Kumar, V., Paraschivoiu, M., & Paraschivoiu, I., Low Reynolds number vertical axis wind turbine for Mars. *Wind Engineering* **34**(4), 461-476 (2010). doi:10.1260/0309-524X.3.4.46.
17. Schorbach, V., & Weiland, T., Wind energy as a backup energy source for Mars missions, *Acta Astron.* **191**, 472-478 (2021). doi:10.1016/j.actaastro.2021.11.013
18. Siemans Gamesa Renewable Energy SG 14-2222 DD, https://www.siemensgamesa.com/en-int/products-and-services/offshore/wind-turbine-sg-14-222-dd. Online: accessed January 30, 2022.
19. Ravikumar, S., Jaswanthvenkatram, V., Sai kumar, Y. J. N. V., & Sohaib, S.Md., Design and analysis of wind turbine blade hub using aluminum alloy AA 6061-T6, *IOP Conf. Ser.: Mater. Sci. Eng.* **197**, 012044 (2017).
20. Okokpujie, I. P., et al., Implementation of multi-criteria decision method for selection of suitable material for development of horizontal wind turbine blade for sustainable energy generation, *Heliyon* **6**(1), e03142. doi:101.1016/j.heliyon.2019.e03142.
21. Bae, J.-S., et al., Preliminary Study on a fabric-covered wind turbine blade, *2015 International Conference on Renewable Energy Research and Applications (ICRERA)*, 1196-1200 (2015). doi: 10.1109/ICRERA.2015.7418598.
22. Dorminey, B., NASA Eyes Tiny Wind Turbines to Power Martian Weather Stations. Forbes (2020) https://www.forbes.com/sites/brucedorminey/2020/08/30/nasa-eyes-tiny-wind-turbines-to-power-martian-weather-stations/?sh=70949eb02c0d.
23. Al-Khayat, M., et al., Performance analysis of a 10-MW wind farm in a hot and dusty desert environments. Part 2: Combined dust and high-temperature effects on the operation of wind turbines.Sustain. Energy Technol. Assess. 47, 101461 (2021). doi:10.1016/j.seta.2021.101461.
24. Manwell, J. F., McGowan, J. G., & Rogers, A. L., *Wind Energy Explained: Theory, Design and Application* (Wiley, ed. 2, 2002).
25. Karnauskas, K. B., Lundquist, J. K., & Zhang, L., Southward shift of the global energy resource under high carbon dioxide emissions. *Nature Geosci.* **11**, 38-43 (2018). doi:10.1038/s41561-017-0029-9,
26. Forte, E., et al., Pressurized brines in continental Antarctica as a possible analogue of Mars. *Sci. Rep.,* **6,** 33158 (2016). doi:10.1038/srep33158.
27. Rucker, M., Integrated Surface Power Strategy for Mars, paper presented at the Nuclear and Emerging Technologies for Space, Albuquerque, NM, 2015. https://ntrs.nasa.gov/citations/20150000526

28. Mozumder, M. S., Mourad, A.-H. I., Pervez, H., & Surkatti, R., Recent developments in multifunctional coatings for solar panel applications: A review, Sol. Energy, 189, 75-102 (2019) doi:10.1016/j.solmat.2018.09.015.
29. Landis, G. A., Dust obscuration of Mars solar arrays. *Acta Astronautica* **38**(11), 885-891, (1996).
30. NASA SBIR 2017 Phase I Solicitation H4.01 Mars Surface Solar Array Structures (2017) https://www.sbir.gov/node/1227185. Online: accessed February 2, 2022.
31. NASA SBIR 2018 Phase I Solicitation H5.01 Mars Surface Solar Array Structures (2018) https://www.sbir.gov/node/1418573. Online: accessed February 2, 2022.
32. NASA SBIR 2019 Phase I Solicitation H6.01 Lunar Surface Solar Array Structures (2019) https://www.sbir.gov/node/1547861. Online: accessed February 2, 2022.
33. Callas, J. L., Golombek, M. P., & Fraeman, A. A., Mars Exploration Rover Opportunity end of mission report; National Aeronautics and Space Administration, Jet Propulsion Laboratory, California Institute of Technology; JPL Publication: Pasadena, CA, USA, p. 56 (2019). http://hdl.handle.net/2014/47103.
34. Kahre, M. A., et al., High resolution modeling of the dust and water cycles with the NASA Ames Mars global climate model. American Geophysical Union, Fall Meeting 2018 (2018).
35. Haberle, R. M., et al., Documentation of the NASA/Ames Legacy Mars Global Climate Model: Simulations of the present seasonal water cycle. *Icarus* **333**, 130-164 (2019). doi:10.1016/j.icarus.2019.03.026.
36. Montabone, L., et al., Eight-year climatology of dust on Mars, *Icarus* **251**, 65-95 (2015). doi:10.1016/j.icarus/2014.12.034.
37. Enercon E33-330 https://www.thewindpower.net/turbine_en_1_enercon_e33-330.php Online: accessed February 3, 2022.
38. Jacobs Wind Electric 31-20 https://en.wind-turbine-models.com/turbines/537-jacobs-wind-electric-31-20 Online: accessed February 3, 2022.
39. Jonkman, J., Butterfield, S., Musial, W., & Scott, G., “Definition of a 5-MW reference wind turbine for offshore system development” (Tech. Rep. NREL/TP-500-38060, NREL, 2009; https://www.nrel.gov/docs/fy09osti/38060.pdf).
40. Aeolos, Aeolos-V Vertical wind turbine brochure, https://www.renugen.co.uk/content/micro_wind_turbine_brochures/micro_wind_turbine_brochures/Aeolos%20Wind%20Turbine/Aeolos-Aeolos-V-300w-300W-Wind-Trubine-Brohcure.pdf Online: accessed February 3, 2022.

Figures

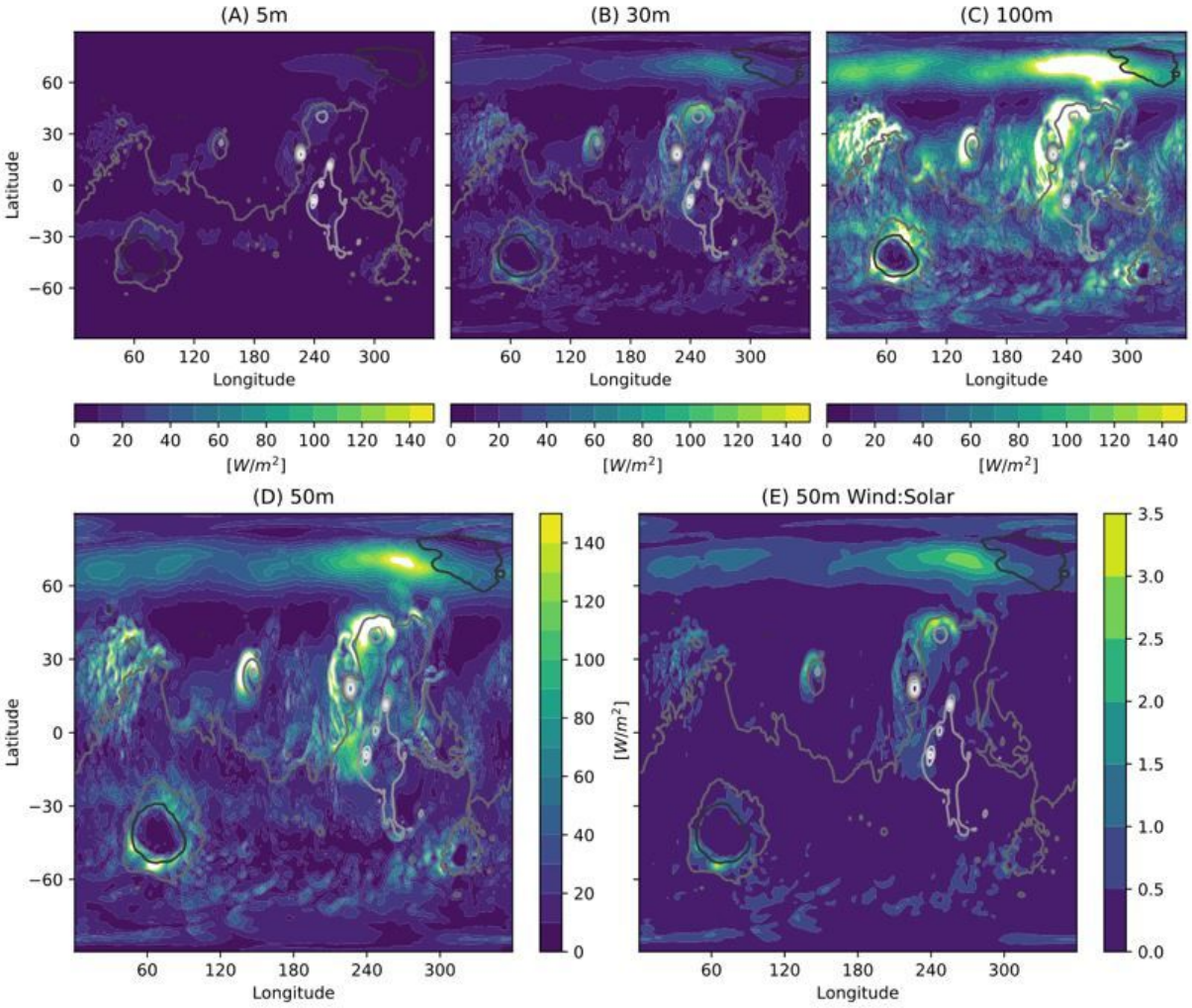

Figure 1

Wind power potential varies with altitude above the surface. At 50m the ratio of wind to solar power can exceed 1. Annual average (MY24) wind power density [W/m^2] at (**A**) 5m, (**B**) 30m, (**C**) 100 m and (**D**) the reference altitude for our base turbine, 50 m above the surface. Panel (**E**) shows the ratio of wind to solar power at 50m. Solid contours in all panels show surface topography.

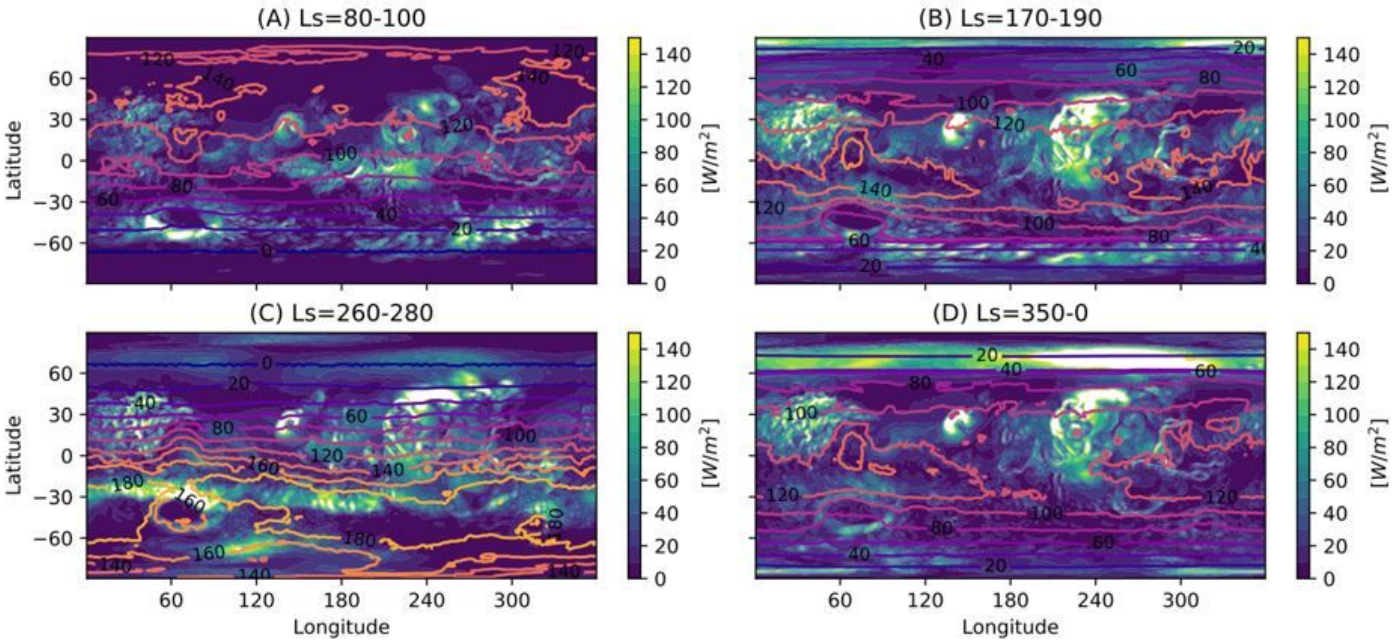

Figure 2

Wind power density exceeds solar power density particularly in the winter hemisphere middle to polar latitudes. Seasonal wind power density [W/m^2] at 50m for the Mars cardinal seasons in 20° L_s bins. Solid contours show the surface solar power density for the same season. Solar power varies latitudinally with season. Baroclinic wave activity adjacent to the winter polar vortex accelerates atmospheric wind speeds when solar energy yields are depleted.

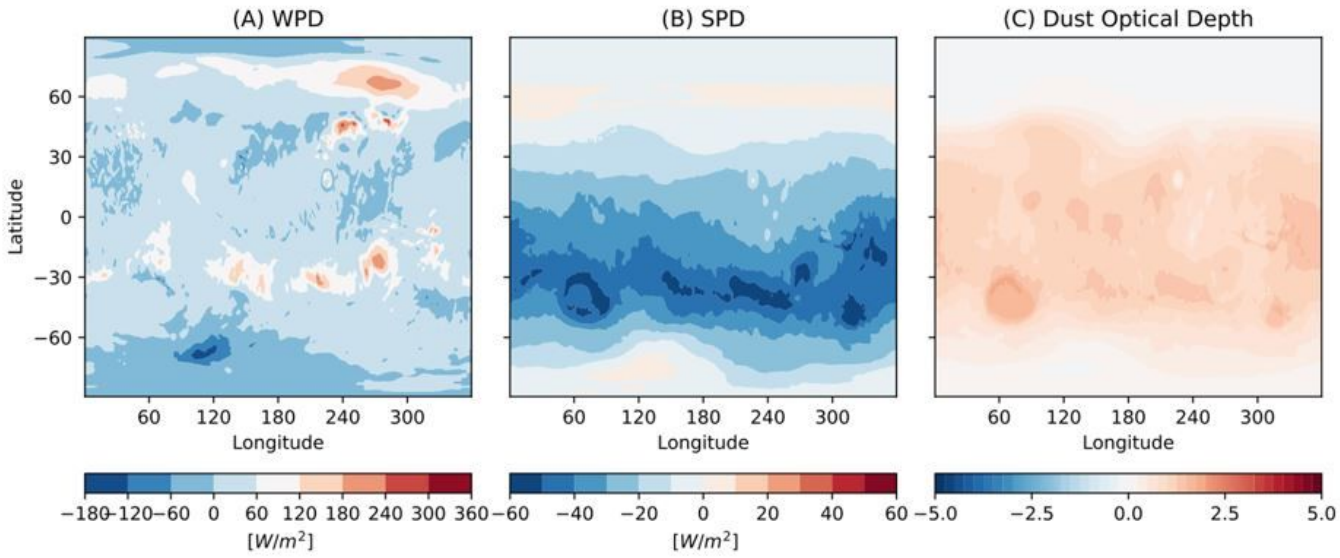

Figure 3

Wind energy increases during global dust storms while solar power is reduced. Difference in (**A**) wind power density, (**B**) solar power density, and (**C**) dust optical depth for a global storm year (MY 28) minus a non-global storm year at perihelion (L_s=260°-280°).

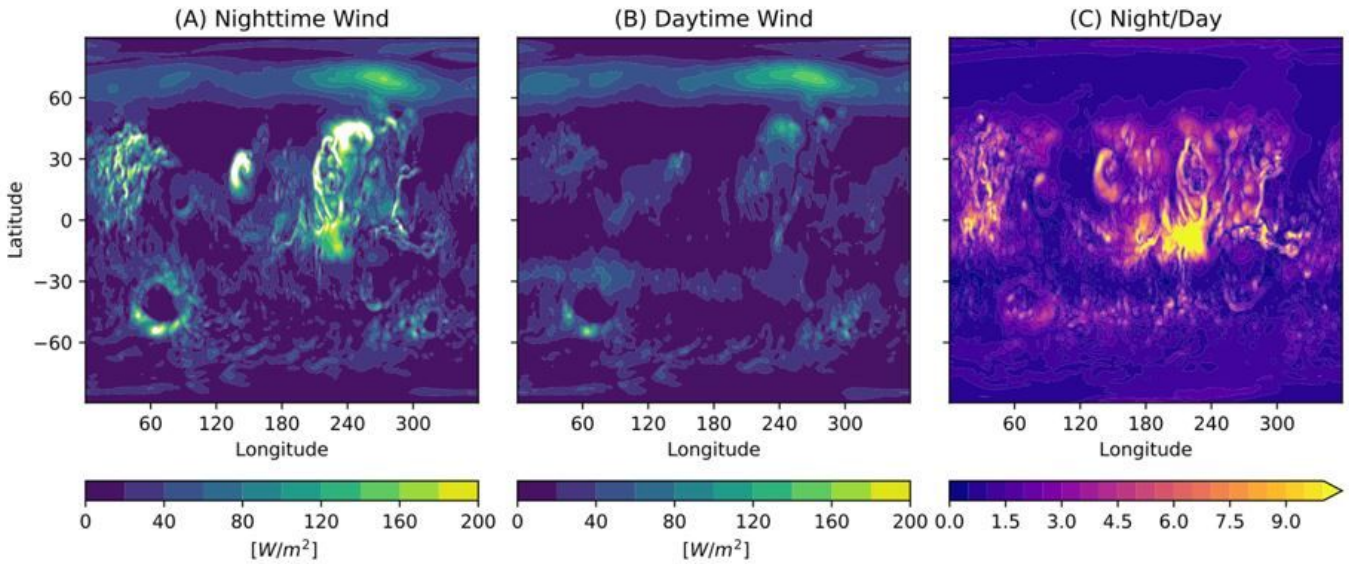

Figure 4

Wind power is greatest at night when solar power is at a minimum. Panels show the annual average (**A**) daytime (7.5-16.5 LT) and (**B**) nighttime wind power density and (**C**) their ratio.

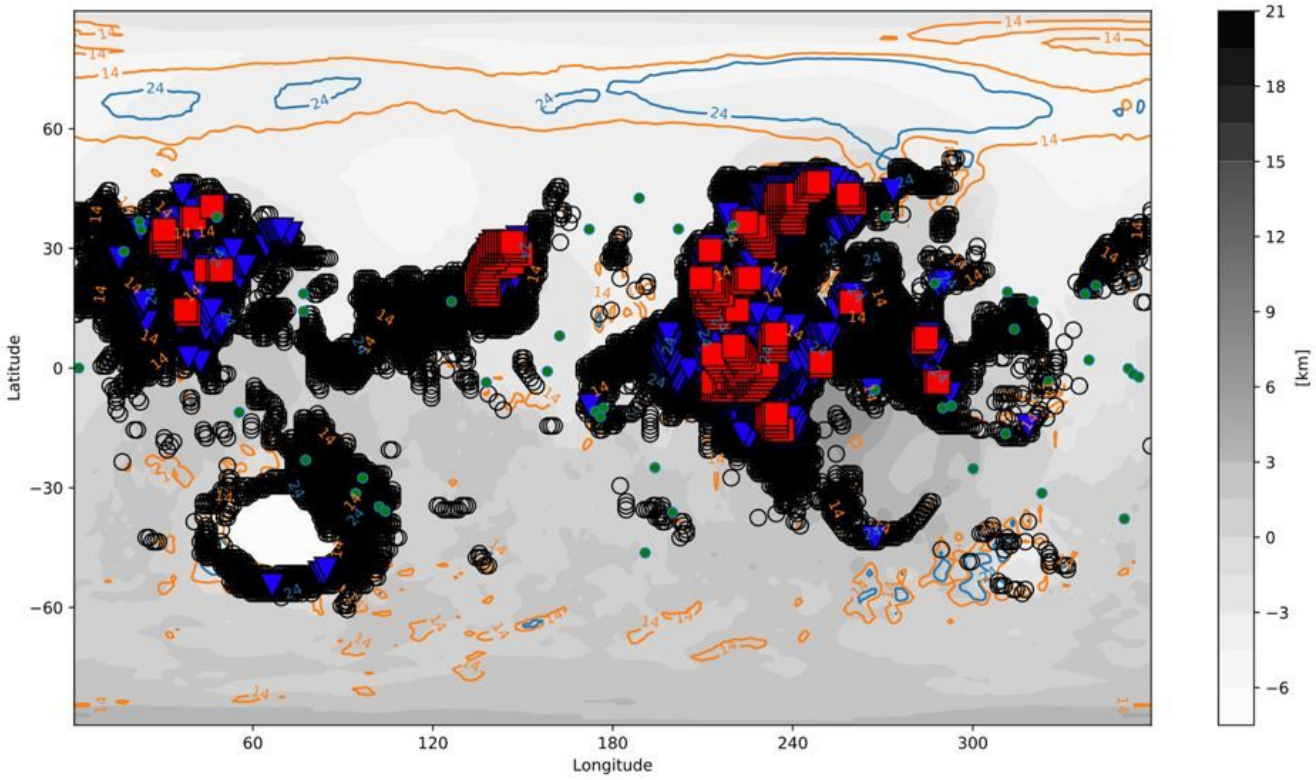

Figure 5

Regions where wind energy could provide power for human missions. Red squares show regions that produce 5-sol diurnal average power levels continuously through a year greater than 24 kW. Blue triangles show regions that could power the life support systems (> 15 kW). Open black circles show regions that could power scientific instrumentation (>2.2 kW)

Solid green circles show proposed landing sites from the NASA HLS2 Workshop. Contour lines show regions where the annual mean wind power production is greater than 14.2 and 24kW. Filled contours show the topography.

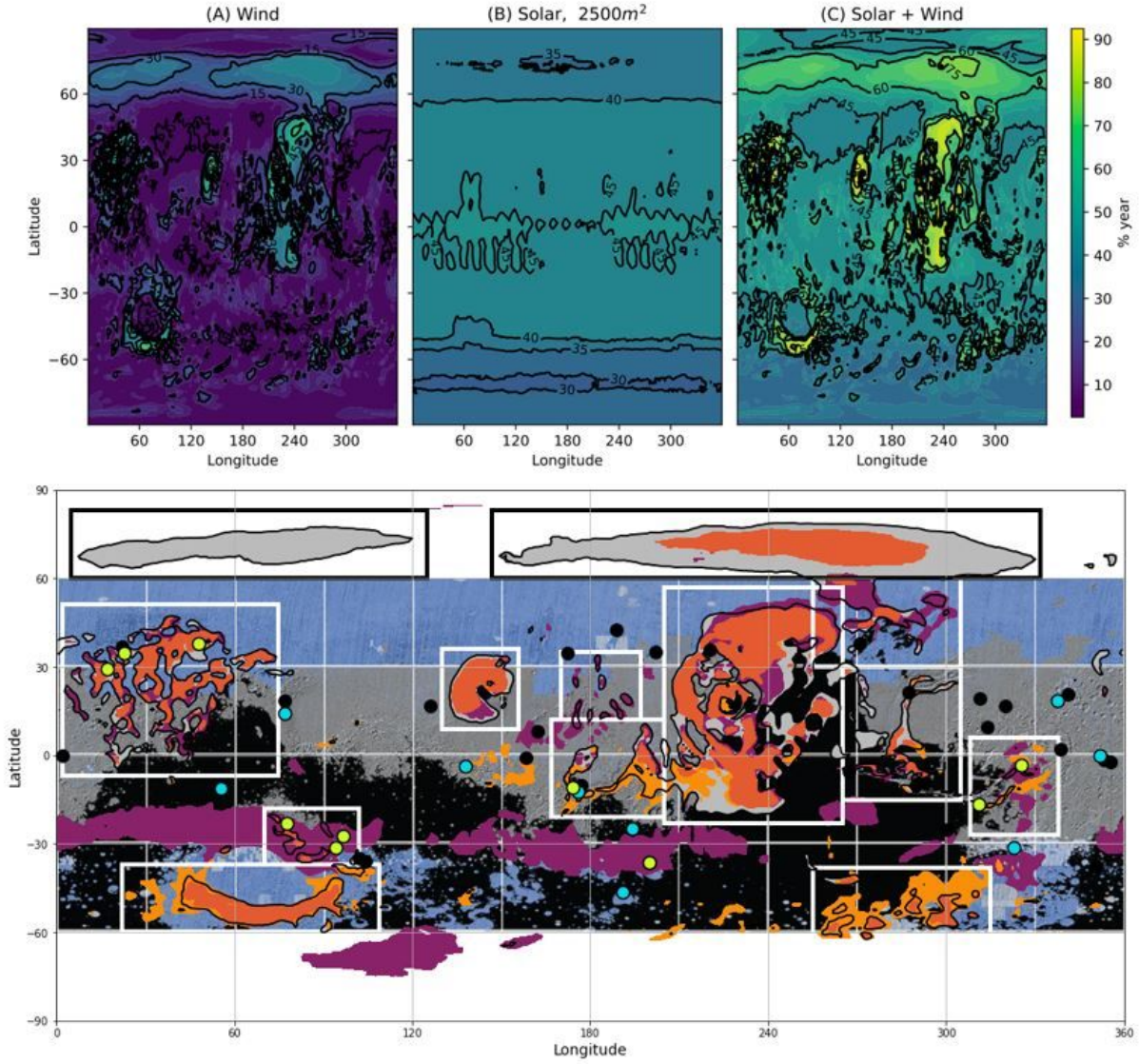

Figure 6

We identify 13 new potential regions of interest where wind power exceeds 24kW for more than 40% of the Mars year (orange contours) or season (L_s=90° light orange, L_s=270° purple). Gray contours show regions where the combined solar and wind power exceeds 24 kW more than 65% of the Mars year. Black and white boxes show newly identified ROI. Yellow circles show ROI that have been specifically flagged for future work based on our analysis (Table S2). Blue circles show crater ROI that may have significant topographic-induced winds and should be studied at higher resolution. The background image shows results from the NASA Subsurface Water Ice Mapping (SWIM) 2.0 Global Products data release (8). Blue regions indicate ice 1-5 m below the surface.

Supplementary Files

This is a list of supplementary files associated with this preprint. Click to download.

- Hartwick2022ExtendedDataNatureAstro.docx